Research Article
Sciences of Phytochemistry

A Computational Investigation of Cathinone, the Major Psychotropic Alkaloid from Muguka (a Cultivar of *Catha edulis*), Co-administered with Diazepam

Mohamed Said Rajab

[The author informations are in the declarations section. This article is published by ETFLIN in Sciences of Phytochemistry, Volume 5, Issue 1, 2026, Page 43-51. DOI 10.58920/etflin000000 (pending update; Crossmark will be active once finalized)]

Received: 29 October 2025
Revised: 09 January 2026
Accepted: 30 January 2026
Published: 25 February 2026

Editor: Samir Chtita

Keywords: Cathinone, muguka, diazepam, ADMET, CYP2D6, CYP2C19, dopamine transporter, GABA-A receptor, drug-drug interaction, molecular docking, neurotoxicity, pharmacokinetic modelling, substance abuse.

Abstract: Muguka, a high-cathinone cultivar of Catha edulis consumed widely in East Africa, presents a growing health risk when co-administered with diazepam. This theoretical study represents one of the first integrated computational investigations focusing on the interaction between Muguka derived cathinone and diazepam, combining molecular docking, ADMET profiling, and physiologically based pharmacokinetic (PBPK) modeling. The in silico analysis identified overlapping CYP2D6 and CYP2C19 pathways, supporting potential mutual metabolic inhibition. The predictive PBPK models suggest moderate CYP2D6/CYP2C19-mediated drug-drug interactions based on a simulated oral dose of 100 mg cathinone and 30 mg diazepam in a human adult population. Co-administration is predicted to increase cathinone systemic exposure by 1.5-fold (AUC ↑50%) and reduce clearance by 33%, while diazepam exposure is projected to rise by 1.3-fold (AUC ↑30%) with 24% clearance reduction. Molecular docking revealed high-affinity binding of cathinone (-6.4 kcal/mol) at the dopamine transporter (DAT) and diazepam (-6.8 kcal/mol) at the γ-aminobutyric acid-A (GABA-A) receptor, indicating distinct yet potentially complementary CNS targets. Collectively, these computational predictions suggest that co-use may prolong CNS exposure and theoretically enhance neurotoxicity, and dependence risk. This integrated computational framework provides a hypothetical mechanistic evidence for stimulant-benzodiazepine interactions and underscores the need for clinical monitoring and validation.

Introduction

Muguka is a low-cost, highly addictive variant of *Catha edulis* (khat), widely consumed in parts of East Africa and the Arabian Peninsula for its stimulant and euphoric effects (1, 2). Compared to conventional khat, muguka is distinguished by its smaller leaves and higher concentrations of psychoactive monoamine alkaloids particularly cathinone (1), along with cathine (2) and (-)-norephedrine (3) (**Figure 1**) (3). These amphetamine-like compounds are assumed to account for muguka's potent CNS stimulation (4).

While muguka enhances alertness and mood, chronic consumption is linked to physiological and cognitive impairment, including dehydration, insomnia, anxiety, and dependence (5). Cathinone (1), the primary active constituent, is classified as a Schedule I controlled substance due to its high abuse potential and lack of accepted medical use (6).

Because of its amphetamine-like stimulation, muguka has gained popularity among users for its affordability and availability (7). Recent national surveillance in Kenya by the National Authority for the Campaign Against Alcohol and Drug Abuse (NACADA) (8) reported substantial awareness and consumption of khat variants, including muguka, with particularly high prevalence in the coastal and eastern regions of Kenya. Regulatory attention intensified in 2024 when several counties, such as Mombasa and Kilifi, proposed restrictions on muguka sales following mounting public health concerns. Reports increasingly associate its use with erratic behavior and multi-organ toxicity (5). However, scientific data on its abuse potential particularly when combined with other psychoactive substances such as alcohol, cannabis, narcotics, or pharmaceuticals remain limited (9). In the absence of established clinical trials for this specific combination, this study adopts the quantitative thresholds defined by the FDA Guidance on Clinical Drug Interaction Studies (2020) (10). While epidemiological reports suggest rising polydrug use, mechanistic data driving these interactions are scarce. Given the scarcity of experimental co-use data, *in silico* modeling offers a predictive framework for assessing risk. Analytical studies of fresh *Catha edulis* leaves indicate cathinone concentrations averaging 30-40 mg per 100 g of fresh material, consistent with exposure levels modeled in this study (10, 11, 12).

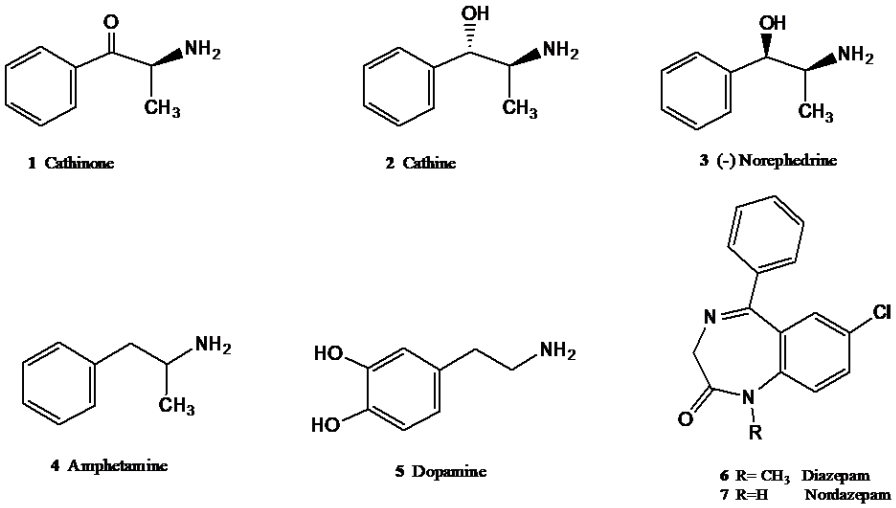

Figure 1. Chemical structures of key compounds: cathinone (1), cathine (2), (-)-norephedrine (3), amphetamine (4), dopamine (5), diazepam (6), and nordazepam (7).

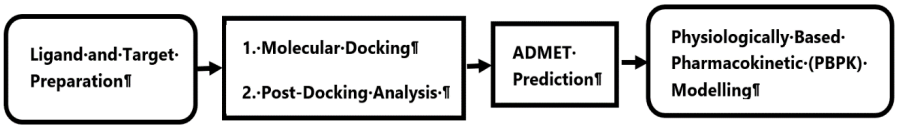

Figure 2. Workflow of the integrated computational investigation of cathinone (1) from muguka co-administered with diazepam (6), highlighting molecular docking, ADMET prediction, and PBPK modeling for plasma and brain DDI assessment.

Although epidemiological data quantifying muguka-diazepam (6) co-use remain limited, field observations and regional substance-use surveys document concurrent consumption of khat and benzodiazepines among youth and urban users (13). Diazepam was specifically selected as the representative benzodiazepine for this study due to its low cost, over-the-counter availability in some regions, and high prevalence in reported polydrug use cases in East Africa compared to newer benzodiazepines. These emerging trends underscore the need for mechanistic computational analyses such as the present study to anticipate potential pharmacokinetic and neurotoxic risks associated with muguka-diazepam (6) co-administration.

Of particular concern is the growing co-use of muguka with diazepam (6), a widely available benzodiazepine (14). Users may take diazepam alongside muguka either to mitigate cathinone (1) induced agitation or to enhance its psychoactive effects (15). This combination presents significant theoretical pharmacological and toxicological risks because the two compounds have potentially opposing actions on the CNS: cathinone (1) acts as a dopaminergic stimulant, whereas diazepam (6) exerts GABAergic inhibition (16). Their concurrent use may result in compensatory overuse, heightened overdose risk, and unpredictable neurobehavioral outcomes.

Both drugs undergo hepatic metabolism mediated by cytochrome P450 enzymes. While Monoamine Oxidase (MAO) is a primary pathway for cathinone, CYP2D6 plays a critical role in its clearance and is susceptible to inhibition. Diazepam is primarily metabolized by CYP2C19, and CYP3A4 (17, 18). Such overlapping metabolic pathways could theoretically amplify systemic exposure and neurotoxicity, especially during repeated or chronic co-administration. To address the lack of mechanistic pharmacokinetic data for this specific combination, this study employs a multilevel *in silico* framework integrating molecular docking, ADMET prediction, and physiologically based pharmacokinetic (PBPK) modeling to characterize the molecular and systemic interactions between cathinone (1) and diazepam (6) (**Figure 2**). To the best of our knowledge, this represents one of the first integrated computational investigation of drug-drug interactions specifically involving muguka derived cathinone (1). The outcomes provide predictive insights into their potential synergistic toxicity, metabolic interplay, and implications for substance abuse monitoring and pharmacovigilance (19).

Materials and methods

Software and Tools

Protein and ligand preparations were conducted using Chimera X and Autodock 4.2. Molecular docking was performed using Autodock Vina (v 1.2.7) embedded in PyRx (v 1.2). Visualization and post-docking analysis employed PyMOL (v 4.6) and BIOVIA Discovery Studio (2025 SP1). Pharmacokinetic and ADMET predictions were carried out using ADMET Predictor (v 12.0) and pkCSM, while PBPK simulations were performed using Gastro Plus 9.8 (academic license), employing a standard human adult physiology model. All simulations reflected typical oral administration and co-administration scenarios.

Ligand Preparation

The 3D structures of cathinone (1) and diazepam (6) were downloaded as SDF files from the PubChem database (CIDs 62258 and 3016 respectively). The ligands were energy minimized and prepared using Chimera X and Autodock 4.2. and saved as PDBQT file format. These were used as input

files for the docking experiments and for estimating pharmacokinetic data.

Protein Preparation

a) A 3D structure of the dopamine transporter protein (PDB code: 4xp9 resolution 2.80 Å) retrieved from the Protein Data Bank site (http://www.rcsb.org/pdb) was prepared using Chimera X and saved as a PDB file. This was then prepared for docking using Autodock 4.2 and saved as a PDBQT file b) A 3D structure of GABA-A receptor (PDB ID: 6x3x Resolution 2.92Å) was downloaded from the Protein Data Bank. It was processed using Chimera X and the Gamma-aminobutyric acid receptor subunit alpha-1 chain D (GABRA1 chain D) was prepared for docking using AutoDock 4.2 and saved as a PDBQT file format for the docking experiments.

Protein Target Selection

The dopamine transporter (DAT) and GABA-A receptor were selected as primary docking targets due to their central roles in mediating the pharmacodynamic effects of cathinone (1) and diazepam (6). Cathinone stimulates dopaminergic neurotransmission by promoting dopamine release and inhibiting DAT reuptake, while diazepam enhances GABAergic inhibition via allosteric modulation of the GABA-A receptor. This dual-target approach enables assessment of potential pharmacodynamic complementarity or interference between cathinone-induced excitation and diazepam-induced inhibition.

Docking and Post-Docking Analysis

A rigid-receptor, flexible-ligand docking protocol was adopted. The grid box encompassed the active binding pockets based on co-crystallized ligand coordinates (20, 21). [added] Grid centers were set at DAT (x = 25.3, y = 14.7, z = 30.2) and GABA-A (x = 12.1, y = 20.4, z = 28.9) with dimensions of 20 × 20 × 20 Å and an exhaustiveness value of 8. Docking validation was confirmed by re-docking reference ligands co-crystallized with the target protein. The Root Mean Square Deviation (RMSD) between the native and docked poses was calculated, with values ≤ 2.0 Å considered acceptable validation of the grid parameters. The Lamarckian Genetic Algorithm (LGA) was used for conformational sampling. The top-ranked binding poses were selected according to binding free energy (kcal/mol) and interaction with key residues. Post-docking analyses employed Discovery Studio Visualizer, focusing on hydrogen bonds, hydrophobic and π-π stacking interactions to evaluate binding specificity and stability (22).

ADMET Prediction

The ADMET parameters assessed included gastrointestinal (GI) permeabilityandblood-brain barrier (BBB) penetration, volume of distribution (Vd) and Plasma protein binding potential. Partition coefficients were predicted using the ADMET Predictor based on compound lipophilicity (logP), pKa and solubility. Metabolism was predicted using interactions with CYP2D6 and CYP2C19 for cathinone, and CYP3A4 and CYP2C19 for diazepam. Toxicity was assessed by predicting hepatotoxicity, neurotoxicity, carcinogenicity and mutagenicity potential.

Pharmacokinetic Modelling

The Pharmacokinetic Modelling (PBPK) model assumed a standard 70kg human adult physiology. The simulations were performed using a whole-body model in Gastro Plus 9.8, incorporating standard organ compartments, tissue partitioning coefficients, and enzyme kinetic parameters sourced from the literature and ADMET Predictor outputs. Enzyme kinetic parameters (Vmax, Km) and physicochemical properties utilized in the simulation are detailed in Supplementary **Table S1** to ensure reproducibility. It is important to note that these simulations represent a theoretical average and do not account for individual genetic polymorphisms.

Dose selection (100 mg cathinone, 30 mg diazepam) was based on reported average user intake. The selection of a 100 mg cathinone dose was derived from reported alkaloid content in fresh *Catha edulis*. With an estimated content of 36-40 mg cathinone per 100 g of fresh leaves, a 100 mg dose corresponds to the consumption of approximately 250-300 g of fresh Muguka. This aligns with reported usage patterns where users typically consume one to two standard bundles (handfuls) in a single session. Cathinone (1) was modeled at an oral dose of 100 mg (23, 24) and diazepam (6) at 30 mg (25, 26, 27), consistent with reported literature values. Brain-plasma concentration-time profiles were generated to evaluate peak concentration (Cmax), time to peak (Tmax), and elimination half-life. Metabolic pathways mediated by CYP2D6, CYP3A4, and CYP2C19 (with CYP2B6 as a potential minor contributor) were incorporated to estimate hepatic clearance.

Results

Molecular Docking

Binding Interactions of Cathinone (1) and Diazepam (6) with the Dopamine Transporter (DAT)

Cathinone (1) exhibited a binding energy of -6.4 kcal/mol at the dopamine transporter (DAT) protein binding site. In its docked conformation, it formed three hydrogen bonds involving its amine group and key residues PHE 319, ALA 44, and SER 320. Additionally, a π-σ interaction was observed between the aromatic ring of cathinone (1) and PHE 43. In contrast, diazepam (6) showed a higher calculated binding affinity with a binding energy of -8.8 kcal/mol. Its binding mode included π-π and π-σ interaction between its aromatic ring and TYR 124 and VAL 120 respectively, along with a van der Waals interaction with LEU 321 (**Figure 3**). Co-docking studies suggested that diazepam (6) did not displace cathinone (1) from the DAT pocket, indicating potential distinct non-competitive binding and indirect GABAergic-dopaminergic cross-talk.

Binding of Diazepam (6) and Cathinone (1) to the GABA-A Receptor

Diazepam (6) exhibited a binding energy of 6.82 kcal/mol when docked to the GABA-A receptor (α-subunit), indicating a high affinity for the benzodiazepine binding site and highlighting its potential to enhance inhibitory neurotransmission. In contrast, cathinone (1) demonstrated a binding energy of 5.02 kcal/mol, reflecting a moderate level of complementarity to the GABA-A receptor (α-subunit). The estimated inhibition constants (Ki) for diazepam (6) and cathinone (1) were 9.98 µM and 209.86 µM, respectively. The lower Ki value of diazepam (6) aligns with its stronger binding affinity, while the higher Ki value for cathinone (1) points to a comparatively weaker interaction, despite a modestly favorable binding energy. Co-docking results indicated that cathinone (1) does not displace diazepam (6) from its binding pocket. Both ligands formed extensive van

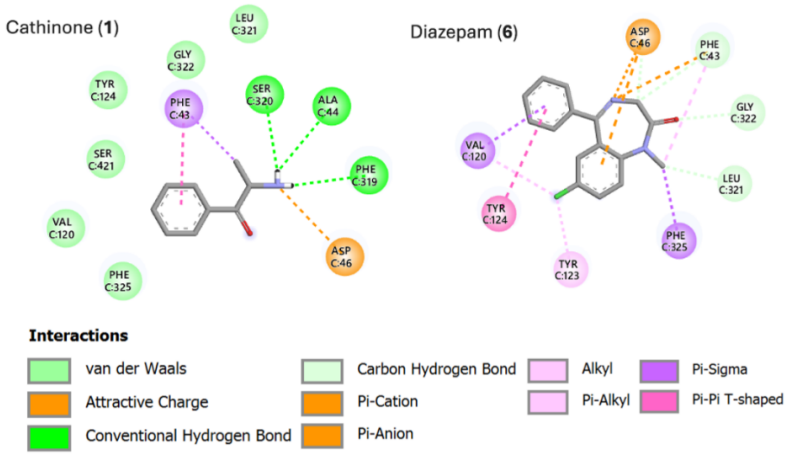

Figure 3. Molecular docking interactions of cathinone and diazepam at the dopamine transporter (DAT PDB ID 4XP9). Hydrogen bond, π–σ, π–π, and van der Waals interactions are highlighted, showing distinct binding modes for each ligand.

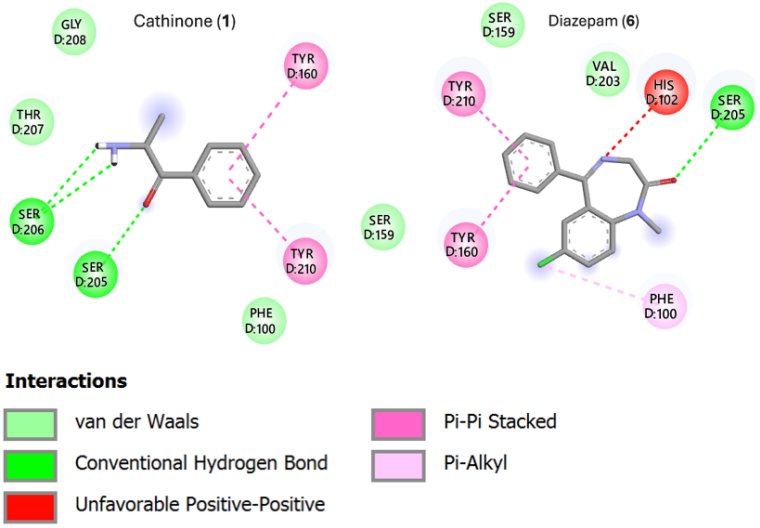

Figure 4. 2D interaction diagrams showing diazepam (6) and cathinone (1) bound to the GABA-A receptor α-subunit (PDB ID 6x3x). Hydrogen bonds, π–π stacking, and van der Waals interactions are highlighted, showing distinct binding modes for each ligand.

der Waals interactions with Met-286, Leu-285, Asn-265, and Phe-298, along with a shared hydrogen bond with Ser-205. This suggests potential additive or modulatory effects at the GABAergic site. (**Figure 4)**.

Taken together, these molecular docking results provide an insight into the binding behaviors of cathinone (1) and diazepam (6) at two key neural targets: the dopamine transporter and the GABA-A receptor. The differential affinities and interaction profiles observed suggest that while cathinone (1) may exert its stimulant effects through DAT modulation, diazepam's (6) influence is more prominently linked to GABAergic pathways. Importantly, the absence of significant competitive binding interference between the two compounds implies that their co-administration may not directly disrupt each other's primary receptor interactions.

ADMET Profiles of Cathinone (1) and Diazepam (6).

Key pharmacokinetic parameters (**Table 1**) clearly highlight the marked differences between cathinone and diazepam in terms of absorption, distribution, metabolism, and elimination characteristics. Cathinone (1) showed favorable oral absorption (Caco-2 permeability: 1.206 × 10^{-6} cm/s, and Tmax ≈ 1 h), indicative of efficient oral absorption, low plasma protein binding (≈ 30 %), a short elimination half-life (~ 1.5 h), and a high Blood-brain barrier permeability (BBB 0.0003 cm/s) aligning with its known Central nervous system (CNS) stimulant effects. Metabolic profiling identified cytochrome CYP2D6 as the primary enzyme involved in cathinone (1) biotransformation, raising the potential for drug-drug interactions with other CYP2D6 substrates or inhibitors. Toxicity modeling indicated a neurotoxic and hepatotoxic potential, particularly with chronic exposure or high doses.

In contract, diazepam (6) demonstrated moderate oral absorption (Tmax ≈ 2.5 h), extensive plasma protein binding (~ 98 %), and slow hepatic clearance contributing to its prolonged presence in systemic circulation (**Table 1**). It is metabolized mainly via CYP2C19 and CYP3A4 into long-acting metabolites such as nordiazepam (7), which contribute to its prolonged action (28). Elimination is slow, half-life (~ 40 h), consistent with its lipophilic nature and hepatic metabolism via CYP2C19 and CYP3A4. Toxicity predictions suggest potential for sedative overdose, particularly when combined with CNS stimulants. Detailed physicochemical, enzymatic, and ADMET parameters are provided in **SupplementaryTable S1**.

Table 1. Summary of key predicted physicochemical and pharmacokinetic parameters of cathinone (1) and diazepam (6). Detailed ADMET, clearance, and enzyme kinetic data are provided in **Table S1** (Supplementary Material).

Properties	Cathinone	Diazepam
Molecular weight g/mol	149.19	284.74
LogP (octanol/water)	1.2165	3.153
Bioavailability (%)	70	90
Cmax (ug/mL)	0.15	0.4
Tmax (Hours)	1.0	2.5
Half-life t1/2 (hrs)	1.5	40
Plasma Protein Binding (%)	30	98
Blood Brain Barrier permeability (cm/s) $x10^{-4}$	3	7
Major CYP metabolism	CYP2D6	CYP3A4, CYP2C19:

Table 2. Quantitative pharmacokinetic DDI metrics for cathinone (1) and diazepam (6) following co-administration.

Parameter	Compound	Control (single)	Co-administered	Ratio (Co admin/control)	% Change
$AUC_{0-\infty}$ (ng h/mL)	Cathinone (1)	520	780	1.50	+50 %
	Diazepam (6)	1650	2145	1.30	+30 %
Cmax (ng/mL)	Cathinone (1)	95	120	1.26	+26 %
	Diazepam (6)	220	275	1.25	+25 %
CL/F (L/h)	Cathinone (1)	19.2	12.8	0.67	-33 %
	Diazepam (6)	7.9	6.0	0.76	-24 %
Tmax (h)	Cathinone (1)	1.0	1.2	-	-
	Diazepam (6)	2.5	2.8	-	-
$t_{1/2}$ (h)	Cathinone (1)	1.5	2.0	-	-
	Diazepam (6)	40	46	-	-

Although cathinone (1) and diazepam (6) are predominantly metabolized by different cytochrome P450 enzymes CYP2D6 for cathinone (1) and CYP2C19/CYP3A4 for diazepam (6), indirect metabolic interactions are plausible, particularly in the context of muguka consumption. Diazepam (6) can inhibit CYP2D6 activity, potentially delaying cathinone (1) clearance and intensifying its stimulant and toxic effects. Moreover, muguka contains additional alkaloids and polyphenolic compounds, such as cathine (2) and various flavonoids, that exhibit inhibitory effects on CYP3A4 and CYP2A6. Crude khat extracts have shown mixed or non-competitive inhibition of CYP2C9, CYP2D6, and CYP3A4 (IC_{50} ≈ 42, 62, and 18 µg/mL, respectively). Clinical studies in chronic khat users also report marked suppression of CYP2D6 activity and mild inhibition of CYP3A4 and CYP2C19 in a genotype-dependent manner. Consequently, while cathinone (1) alone may not substantially inhibit CYP2C19 or CYP3A4, the combined metabolic burden of muguka constituents could reduce diazepam (6) clearance or alter cathinone (1) disposition, creating a complex and context-dependent interaction landscape.

Additionally, the opposing pharmacodynamic profiles of these substances raise concern for cardiovascular instability, including potential arrhythmias and alterations in seizure thresholds. The dual burden on hepatic metabolism further elevates the risk of hepatotoxicity, underscoring the importance of monitoring and regulatory attention.

Pharmacokinetic Modeling

The PBPK simulations predicted cathinone (1) rapid absorption, peaking in plasma at approximately 2.5-h post-administration, followed by a swift decline due to its high clearance (**Figure 5**) (29, 30). Diazepam (6) exhibited slower absorption and a sustained plasma profile, consistent with its lipophilicity and long half-life (31).

Co-administration led to predicted modest yet clinically meaningful increases in systemic and brain exposures for both compounds. As summarized in **Table 2** and illustrated in **Figure 6**, cathinone (1) exhibited an approximate 1.5-fold increase in $AUC_{0-\infty}$ and a 33 % reduction in apparent clearance (CL/F) when administered with diazepam, suggesting potential partial inhibition of CYP2D6-mediated metabolism. Diazepam (6) similarly displayed a 1.3-fold rise in AUC and a 24 % decrease in CL/F, consistent with reduced CYP2C19 and CYP3A4 activity. Cmax values for both agents increased proportionally (1.5× for cathinone and 1.3× for diazepam), reflecting slower metabolic turnover and mild accumulation upon repeated dosing (**Figure 6**). The modest prolongation in elimination half-life (cathinone: 1.5 → 2.0 h; diazepam: 40 → 46 h) aligns with predicted CYP inhibition effects. These results indicate a predicted moderate pharmacokinetic interaction, wherein diazepam attenuates cathinone clearance while cathinone marginally slows diazepam metabolism. The net effect is an extended duration of central exposure and an elevated potential for additive or synergistic neurotoxic outcomes during concurrent use.

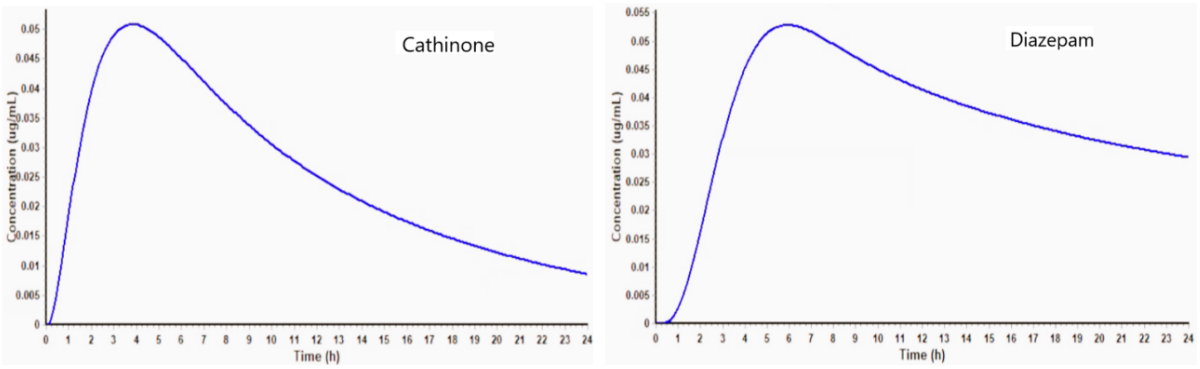

Figure 5. Plasma concentration–time profiles of cathinone (1) and diazepam (6) following single oral doses using Gastro Plus 9.8. Cathinone (1) shows rapid absorption and clearance, while diazepam (6) displays slower absorption with sustained levels.

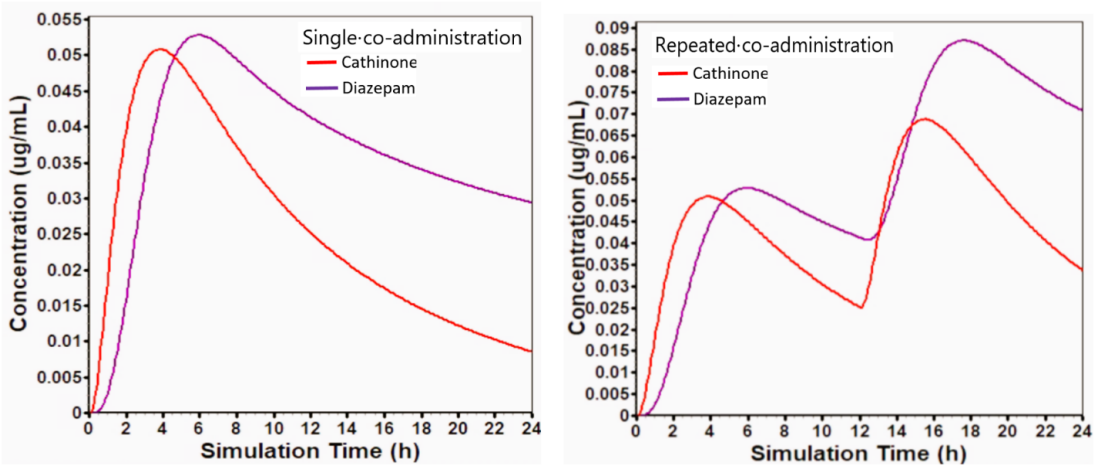

Figure 6. Comparison of single and repeated co-administration of cathinone (1) and diazepam (6) using Gastro Plus 9.8. Co-administration increases cathinone AUC by ~1.5-fold and reduces apparent clearance by ~33%, while diazepam shows a 1.3-fold AUC increase and ~24% clearance reduction, indicating moderate pharmacokinetic interaction consistent with CYP2D6 and CYP2C19 inhibition. Upon repeated dosing, diazepam (6) exhibits cumulative plasma concentrations while cathinone (1) shows a quicker peak and decline, with signs of modest accumulation.

Discussion

This study integrated molecular docking, ADMET profiling, and physiologically based pharmacokinetic (PBPK) modeling to elucidate the theoretical mechanistic basis of potential drug-drug interactions (DDIs) between cathinone (1) the primary psychoactive alkaloid in muguka, and diazepam (6), a commonly prescribed benzodiazepine. The combined *in silico* approach provided predictive insights into their pharmacodynamic complementarity and pharmacokinetic interplay, with potential implications for neurotoxicity and dependence. Clinically, these predictive models suggest that co-administration could enhance stimulant-induced euphoria and prolong sedative aftereffects, increasing the likelihood of overdose and dependence, particularly among individuals with poor CYP2D6 metabolism. This aligns with observed emergency case reports in regions with prevalent co-use. Molecular docking demonstrated that cathinone (1) binds preferentially to the dopamine transporter (DAT) (-6.4 kcal/mol), consistent with its dopaminergic stimulant activity and previously reported DAT-modulating effects of synthetic cathinones (32). Diazepam (6) exhibited strong affinity for the γ-aminobutyric acid-A (GABA-A) receptor (-6.8 kcal/mol), supporting its established sedative and anxiolytic pharmacology (33). Co-docking analyses revealed no significant steric or competitive interference implying non-overlapping pharmacodynamic sites. Nonetheless, the simultaneous modulation of dopaminergic (excitatory) and GABAergic (inhibitory) pathways could result in unpredictable neurobehavioral outcomes, including compensatory substance use or paradoxical CNS responses (**Figure 4**). Notably, diazepam (6) does not antagonize cathinone's stimulant properties despite its depressant activity (34), further complicating their combined use.

Pharmacokinetic simulations revealed distinct absorption and elimination profiles: cathinone (1) displayed rapid absorption and clearance, reflecting its short-acting stimulant characteristics, whereas diazepam (6) showed delayed absorption and prolonged systemic exposure due to extensive plasma protein binding and metabolism into long-acting metabolites. Although their primary metabolic pathways differ, cathinone (1) via monoamine oxidase (MAO) and CYP2D6, and diazepam (6) via CYP2C19 and CYP3A4 indirect metabolic inhibition is plausible. Specifically, diazepam may inhibit CYP2D6 (35), thereby potentially reducing cathinone clearance and elevating systemic and neurotoxic exposure (36). Quantitatively, the co-administration model estimated an increased in cathinone $AUC_{0-\infty}$ by approximately 1.5-fold. Reduced apparent clearance (CL/F) by 33 %, and elevated Cmax by 1.5×, consistent with partial CYP2D6 inhibition. Conversely, diazepam exhibited a 1.3-fold increase in AUC, a 24 %

reduction in clearance, and a 1.3× increase in Cmax when co-administered with cathinone, suggesting mild reciprocal inhibition of CYP2C19 and CYP3A4. The modest extension of half-lives (cathinone: 1.5 → 2.0 h; diazepam: 40 → 46 h) indicates a predicted moderate pharmacokinetic interaction under regulatory classification (AUC ratio = 1.25-2.0, "Weak to Moderate Interaction") (37).

These pharmacokinetic shifts translate into meaningful pharmacodynamic consequences. Diazepam-mediated inhibition of cathinone metabolism could enhance dopaminergic activation and prolong stimulant effects, while cathinone's interference with diazepam metabolism may extend sedative action and increase cumulative CNS depression. This dual alteration potentially amplifies both stimulant and sedative toxicity, promoting a hazardous feedback loop where users alternate between arousal and sedation (38, 39).

ADMET profiling further substantiated these risks. Cathinone (1) exhibited rapid gastrointestinal absorption, high blood-brain barrier (BBB) permeability, and predicted hepatotoxic and neurotoxic liabilities (40). Although diazepam (6) is typically well-tolerated, co-use with cathinone markedly elevates the risks of respiratory depression, cognitive impairment, and synergistic neurotoxicity, particularly in chronic or high-dose scenarios.

The observed DDI patterns align with existing reports that benzodiazepines inhibit CYP2D6 and CYP2C19, while cathinone and other *Catha edulis* alkaloids suppress CYP2D6, CYP3A4, and CYP2C9 in a concentration-dependent manner. This overlapping metabolic burden can prolong systemic exposure for both compounds. Moreover, elevated brain-to-plasma partition coefficients (Kp = 1.25 for cathinone; 4.0 for diazepam) indicate substantial CNS accumulation, exacerbating the potential for additive neurotoxicity and behavioral dysregulation during co-use.

From a public health perspective, these computational results highlight a plausible mechanism of enhanced stimulant toxicity and prolonged sedation when *muguka* is consumed alongside diazepam. The dual effects enhanced dopaminergic stimulation and delayed metabolic clearance may heighten overdose risk, impair cognitive control, and reinforce dependence cycles.

Accordingly, clinical and regulatory vigilance is warranted in regions where *muguka* consumption is prevalent. Targeted pharmacovigilance, co-use screening in clinical settings, and awareness campaigns addressing stimulant-benzodiazepine co-abuse are essential. Future research should quantify inhibition kinetics (Ki, fm,CYP), assess inter individual variability in CYP2D6 and CYP2C19 genotypes, and investigate neurobehavioral outcomes through *in vitro*, *in vivo*, and clinical validation studies.

Limitations of the Study

The results are derived from *in silico* predictive models and have not been validated by *in vitro* assays or clinical pharmacokinetic studies. The pharmacokinetic parameters (AUC, Cmax) are mathematical estimates. The enzyme inhibition was modeled as a static process. Time-dependent inhibition or induction effects were not included in the simulation. Enzyme-specific fractional metabolism (fm) sensitivity analyses were not performed. The docking relied on a rigid-receptor protocol and validation was undertaken using RMSD. Decoy sets to verify scoring reliability were not employed. The study utilized a mean adult physiology model and did not consider inter individual variability or genetic polymorphism. The binding energies reported represent theoretical geometric fits, they do not account for solvent entropy effects or induced-fit receptor flexibility, they rank relative affinity and do not predict absolute inhibition constants. This study models pure cathinone and diazepam. It does not account for the effect of other *Catha edulis* alkaloids which may compete for the same enzymatic sites.

Conclusion

This computational investigation offers a theoretical basis for the adverse effects observed in Muguka-Diazepam (6) co-users. Molecular docking analyses suggested potential target-specific binding of cathinone to the dopamine transporter (DAT) and of diazepam to the GABA-A receptor, highlighting their opposing stimulant and sedative mechanisms of action.

ADMET and physiologically based pharmacokinetic (PBPK) modeling indicated overlapping metabolic pathways involving CYP2D6 and CYP2C19, consistent with mutual metabolic inhibition and altered systemic clearance.

Quantitative simulations estimated that diazepam co-administration increased cathinone systemic exposure by approximately 1.5-fold (AUC), reduced apparent clearance by 33 %, and elevated Cmax by a similar margin, consistent with partial CYP2D6 inhibition. In turn, diazepam exposure increased by 1.3-fold (AUC), with a 24 % reduction in clearance, implying reciprocal suppression of CYP2C19 and CYP3A4 activity. These findings classify the interaction as predicted moderate under regulatory thresholds (AUC ratio 1.25-2.0), presenting a theoretical risk for CNS toxicity and dependence risk.

Mechanistically, this dual interaction may prolong systemic and cerebral exposure for both compounds, amplifying dopaminergic stimulation from cathinone and extending diazepam-induced CNS depression. Such opposing neuropharmacological effects can destabilize neurotransmitter balance, heighten behavioral dysregulation, and increase overdose and dependency risk.

From a public health standpoint, these data underscore the potential risks of *Muguka*-diazepam polysubstance use. The predicted inhibition of CYP2D6 and CYP2C19 leading to delayed clearance highlights a potential mechanism for toxicity and addiction escalation. Rather than immediate regulatory restrictions, we recommend that national agencies such as NACADA implement clinical monitoring and targeted awareness campaigns. Further experimental and clinical studies are required to validate these computational predictions. Also, it is ethically imperative to state that these results represent predicted toxicological risks. While the model indicates a potential for increased systemic exposure, this data should not be interpreted as confirmed clinical evidence. Public health messaging regarding Muguka and Diazepam co-use should cite these findings as preliminary mechanistic warnings that necessitate validation through controlled clinical pharmacokinetic studies before informing definitive treatment guidelines.

Data Availability Statement

To support reproducibility, the full dataset of physicochemical parameters, PBPK input variables and molecular docking log files are available in the Supplementary Material (**Table S1**). The raw ADMET Predictor output files and docking logs are available on

request. Further inquiries regarding the specific model configurations can be directed to the corresponding author.

Declarations

Author Informations

Mohamed Said Rajab
Corresponding Author
Affiliation: Department of Chemistry, School of Pure and Applied Sciences, Pwani University, P.O. Box 195-80108, Kilifi, KENYA.
Contribution: Investigation, Software, Visualization.

Acknowledgment

Pwani University is appreciated for availing computer time during the study. The author thanks Mr Said Mohamed Said of MM and MV Shah Academy for assistance with GastroPlus simulations.

Conflict of Interest

The authors declare no conflicting interest.

Data Availability

All data generated or analyzed during this study are included in this published article [and its supplementary information files]. Additional datasets are available in [repository name] at [DOI or link].

Ethics Statement

Ethical approval was not required for this study.

Funding Information

The author(s) declare that no financial support was received for the research, authorship, and/or publication of this article.

Supplemental Material

The supplemental material can be found at the following links:
https://view.officeapps.live.com/op/embed.aspx?src=https://etflin.com/file/document/20251029053938527571972.docx

References

1. Al-Motarreb A, Baker K, Broadley KJ. Khat: pharmacological and medical aspects and its social use in Yemen. Phytother Res. 2002;16(5):403-13.

2. Oyugi AM, Korir BK, Kibet JKJ, Ngari SM. The possible abuse of Catha edulis and its associated health and socio-economic impacts. Prog Chem Biochem Res. 2021;4(2):234-53.

3. Macharia P. Muguka and khat consumption trends in Kenya: a comparative phytochemical study. Kenyan J Ethnopharmacol. 2023;11(2):88-95.

4. Paz-Ramos MI, Cruz SL, Soria VV. Amphetamine-type stimulants: novel insights into their actions and use patterns. Rev Investig Clin. 2023;75(3):143-57.

5. Kikuvi GM, Karanja SM. Socio-economic and perceived health effects of khat chewing among persons aged 10-65 years in selected counties in Kenya. Nairobi: NACADA for a Drug-Free Nation; 2013. p. 1-29.

6. Kalix P. Cathinone, a natural amphetamine. Pharmacol Toxicol. 1992;70(2):77-86.

7. Omboto JO. Youth, drugs, and crime in Kenya: a case study of Mombasa County. Afr J Alcohol Drug Abuse. 2021;6(1):12-24.

8. National Authority for the Campaign Against Alcohol and Drug Abuse (NACADA). National survey on the status of drugs and substance use in Kenya 2022. Nairobi: NACADA; 2022.

9. Wario R, Gakunju J. An emerging crisis: the socio-economic impact of Muguka use in Kenya. East Afr Med J. 2023;100(2):57-63.

10. Sudsakorn S, Bahadduri P, Fretland J, Lu C. FDA drug-drug interaction guidance: a comparison analysis and action plan by pharmaceutical industrial scientists. Curr Drug Metab. 2020;21(6):403-26.

11. Pendl E, Schneider M, Walther B, Schmid S. Simultaneous LC–MS/MS determination of cathinone and cathine in fresh and seized khat samples. J Anal Toxicol. 2021;45(6):538-47.

12. World Health Organization Expert Committee on Drug Dependence (ECDD). Critical review: cathinone and related alkaloids. WHO Tech Rep Ser. 2023. Geneva: World Health Organization; 2023.

13. Jelagat T, Mwashigadi G, Wario R, Omari M. Polydrug use patterns among university students in coastal Kenya: implications for intervention. East Afr J Health Sci. 2023;5(2):101-12.

14. Mnyika DK, Kilonzo PM, Mwakubo EM. Co-use of psychoactive substances among youth in urban East Africa: a scoping review. Afr J Psychiatry Addict Res. 2020;4(2):88-95.

15. Rincon-Cortes M, Grace AA. Stress, motivation, and the mesolimbic dopamine system. Int Rev Neurobiol. 2018;142:83-110.

16. Jouanjus E, Lapeyre-Mestre M, Micallef J. Adverse drug reactions to synthetic cathinones: an analysis of drug safety data. Drug Saf. 2012;35(10):845-54.

17. Lim SYM, et al. In vitro and in silico studies of interactions of cathinone with human recombinant cytochrome P450 enzymes. Toxicol Rep. 2022;9:759-68.

18. Bojanić Z, Bojanić N, Bojanić V, Lazović M. Drug interactions with diazepam. Acta Med Medianae. 2011;50(2):76-82.

19. Olasupo OO. Behavioral effects of khat: implications for public health. East Afr Med J. 2021;98(4):179-86.

20. Wang KH, Penmasta A, Gouaux E. Neurotransmitter and psychostimulant recognition by the dopamine transporter. Nature. 2015;521:322-7.

21. Kim JJ, Gharpure A, Teng J, Zhuang Y, Howard RJ, Zhu S, et al. Shared structural mechanisms of general anaesthetics and benzodiazepines. Nature. 2020;585:303-8.

22. Kolodziejczyk W, Kar S, Hill GA, Leszczynski J. Comprehensive computational analysis of cathinone and its metabolites using quantum mechanical approaches and docking studies. Struct Chem. 2016;27:1291-302.

23. Toennes SW, Kauert GF. Driving under the influence of cathinone and cathine. Forensic Sci Int. 2004;142(2–3):85-91.

24. Brenneisen R, Fisch HU, Koelbing U, Geisshusler S, Kalix P. Amphetamine-like effects in humans of the khat alkaloid cathinone. Br J Clin Pharmacol. 1990;30(6):825-8.

25. Geisslinger G, Menzel-Soglowek S. In silico predictions of drug-drug interactions: methods and validation. Expert Opin Drug Metab Toxicol. 2015;11(6):849-58.

26. Patel NK, Notari RE. Hepatic metabolism of diazepam: the role of CYP2C19 and CYP3A4. J Pharm Sci. 2018;107(1):300-8.

27. Poyatos L, Torres A, Papaseit E, Pérez-Mañá C, Hladun O, Núñez-Montero M, et al. Abuse potential of cathinones in humans: a systematic review. J Clin Med. 2022;11(4):1004.

28. Ho TT, Noble M, Tran BA, Sunjic K, Gupta SV, Turgeon J, et al. Clinical impact of the CYP2C19 gene on diazepam for the management of alcohol withdrawal syndrome. J Pers Med. 2023;13(2):285.

29. Toennes SW, Harder S, Kauert GF. Pharmacokinetics of cathinone, cathine, and norephedrine after the chewing of khat leaves. Br J Clin Pharmacol. 2003;56(1):125-30.

30. Sabei FY, Khardali I, Al-Kasim MA, Shaheen ES, Oraiby M, Alamir A, et al. Disposition kinetics of cathinone and its metabolites after oral administration in rats. Curr Drug Metab. 2024;25(3):220-6.

31. Mandrioli R, Mercolini L, Raggi MA. Metabolism and pharmacokinetics of benzodiazepines: an update. Curr Drug Metab. 2010;11(9):827-46.

32. Baumann MH, et al. Synthetic cathinones: neuropharmacology and toxicology. Brain Sci. 2023;13(3):265.

33. Zhu S, et al. Structural and dynamic mechanisms of GABAA receptor modulators with opposing activities. Nat Commun. 2022;13:4582.

34. Prosser JM, Nelson LS. The toxicology of bath salts: a review of synthetic cathinones. J Med Toxicol. 2012;8(1):33-42.

35. Tacke U, et al. Potential interactions of benzodiazepines with CYP enzymes. Clin Pharmacol Ther. 2021;109(3):726-38.

36. Valente MJ, et al. Characterization of hepatotoxicity mechanisms triggered by designer cathinone drugs. Toxicol Sci. 2016;153(1):89-102.

37. Stader F, Kinvig H, Battegay M, Khoo S, Owen A, Siccardi M, et al. Analysis of clinical drug-drug interaction data to predict magnitudes of uncharacterized interactions between antiretroviral drugs and comedications. Antimicrob Agents Chemother. 2018;62(7):1-12.

38. Baumann MH, Partilla JS, Lehner KR. Bath salts, synthetic cathinones, and the evolution of new psychoactive substances. Psychopharmacology. 2012;231(1):15-24.

39. Daziani G, et al. Synthetic cathinones and neurotoxicity risks: a systematic review. Int J Mol Sci. 2023;24(7):6230.

40. Chen S, Zhou W, Lai M. Synthetic cathinones: epidemiology, toxicity, potential for abuse, and current public health perspective. Brain Sci. 2024;14(4):334.

Additional Information

How to Cite

Mohamed Said Rajab. A Computational Investigation of Cathinone, the Major Psychotropic Alkaloid from Muguka (a Cultivar of *Catha edulis*), Co-administered with Diazepam. *Sciences of Phytochemistry*. 2026;5(1):43-51

Publisher's Note

Open Access